Influence of Velocity on Hydrodynamic Flow Characteristics around Subsea Pipelines: A Numerical Analysis

Luh Putri Adnyani[1*], Hifzul Anwar Siregar[2], Samsu Dlukha Nurcholik[3], Destyariani Liana Putri[4]

(Received: 15 August 2025 / Revised: 20 August 2025 /Accepted: 22 August 2025 / Available Online: 12 September 2025)

***Abstract*— This study investigates the influence of flow velocity on hydrodynamic flow characteristics around free-span subsea pipelines using computational fluid dynamics (CFD). Simulations were conducted at flow velocities of 1.1 m/s, 2.5 m/s, and 3.0 m/s to examine changes in the mean flow field, bed shear stress, pressure distribution, and wake development. Results show that increasing velocity transitions the wake from stable laminar to turbulent with fully developed vortex streets, intensifying vortex shedding, wake asymmetry, and unsteady forces. Higher velocities significantly amplify peak bed shear stress, adverse pressure gradients, and the depth of velocity deficits, leading to prolonged wake recovery and increased turbulence. These effects have critical implications for vortex-induced vibration (VIV), hydrodynamic loading, and scour potential, emphasizing the need to consider velocity variation in subsea pipeline design and integrity assessment.**

Keywords— Subsea Pipeline, CFD, Flow Velocity, Vortex Shedding, Hydrodynamic Forces, Wake Dynamics, Bed Shear Stress

*Corresponding Author:luhputria@lecturer.itk.ac.id

I. INTRODUCTION

Subsea pipelines are critical components of offshore infrastructure, used to transport oil, gas, and other materials from offshore platforms to onshore facilities [1]. Understanding the hydrodynamic behavior around these pipelines is essential for their design, stability, and performance [2, 3]. Among the key factors influencing the hydrodynamic forces acting on subsea pipelines is the velocity of the surrounding fluid [4-6]. The flow velocity around the pipeline significantly affects the forces such as drag, lift, and the induced vortex shedding that can lead to structural vibrations and, in extreme cases, pipeline failure. Therefore, understanding the relationship between flow velocity and hydrodynamic forces is crucial for designing pipelines that can withstand the challenging subsea environment.

In subsea pipeline design, the flow velocity plays a critical role in determining the stability of the pipeline and the forces exerted on its structure. The drag and lift coefficients, which are essential to evaluating the pipeline's interaction with the fluid, are highly sensitive to changes in flow velocity. Increased flow velocity can lead to higher drag forces, increased vortex shedding intensity, and greater potential for vibration-induced fatigue. Conversely, the flow may become more stable at lower velocities, resulting in reduced dynamic forces. The velocity's influence on the vortex-induced vibrations (VIV) is significant for free-span pipelines, where sections of the pipeline are unsupported, and the pipeline is more susceptible to hydrodynamic instabilities [7-10].

Luh Putri Adnyani, Institut Teknologi Kalimantan. Email: luhputria@lecturer.itk.ac.id
Samsu Dlukha Nurcholik, Naval Architecture, Insititut Teknologi Kalimantan. Email: dlukha@lecturer.itk.ac.id
Destyariani Liana Putri, Marine Engineering, Institut Teknlogi Kalimantan. Email: putridestyariani@lecturer.itk.ac.id

Flow velocity also affects the symmetry of vortex shedding around the pipeline. At higher velocities, vortex shedding is typically more intense and asymmetric, leading to unsteady forces that can induce oscillations and vibrations in the pipeline. The oscillating forces caused by vortex shedding can cause fatigue damage over time, which is a significant concern for subsea pipelines, particularly those in regions with strong currents. As the velocity decreases, vortex shedding tends to become more symmetrical, which can result in less intense forces acting on the pipeline. The understanding of this relationship between velocity and vortex shedding is vital for mitigating the risks associated with subsea pipeline operations [11-13]. Jensen, et al. [12] investigated the flow around a pipeline using experimental methods and found the lift coefficient ranged from -0.21 to -0.50 and the Strouhal number ranged from 0.17 to 0.36.

The dynamics of hydrodynamic forces on subsea pipelines also depend on the interaction between the flow velocity and other parameters such as the angle of attack of the flow, pipe diameter, and surface roughness. Variations in the heading angle of the flow relative to the pipeline can significantly alter the vortex shedding patterns and the resultant hydrodynamic forces. A comprehensive study of these interactions is required to assess the impact of flow velocity in real-world subsea environments. For example, a pipeline exposed to flow at different angles may experience varying levels of lift and drag forces, which are critical for predicting its long-term stability.

Previous studies investigated flow around a cylinder using experimental data [14], including flow around a span shoulder of a pipeline [15]. In addition, computational fluid dynamics (CFD) simulations provide valuable insights into the complex behavior of fluid flow around subsea pipelines under various conditions [16-21]. These simulations enable the visualization of vortex shedding patterns, flow velocities, and the resulting hydrodynamic forces. By varying the flow velocity and other parameters in a CFD model, predicting the pipeline's response to different operational conditions is possible. Such models are essential for optimizing subsea pipelines' design and operational parameters, ensuring that they can handle dynamic forces without compromising structural integrity. Liang, et al. [22] numerically investigated the scale effect caused by the pipe Reynolds number. It is found that regular vortex movement is observed where Reynolds number is in the subcritical range (300<Re<3x105), while no vortex shedding is predicted in the supercritical range ($3.5x10^5$<Re<$1.5x10^6$).

Experimental studies have also been conducted to validate the theoretical and numerical findings regarding the effect of flow velocity on subsea pipeline behavior. Physical models of subsea pipelines subjected to controlled flow conditions allow researchers to observe real-world vortex shedding and hydrodynamic interactions. These experiments provide valuable data for improving CFD models and refining pipeline design standards. For example, the data collected from model tests can be used to calibrate numerical models, providing more accurate predictions of pipeline behavior under varying flow velocities.

Despite extensive research into the effects of flow velocity on subsea pipeline dynamics, challenges remain in understanding the full spectrum of hydrodynamic interactions. Variability in environmental conditions such as temperature, salinity, and current patterns complicates the prediction of hydrodynamic forces. Therefore, continued research is necessary to develop more robust models to account for these factors and improve the safety and efficiency of subsea pipeline operations. This research will provide a foundation for better pipeline designs and maintenance strategies that reduce the risk of damage from hydrodynamic forces.

In conclusion, the influence of velocity on the hydrodynamic flow around subsea pipelines is a critical factor in their design and operation. Understanding how flow velocity affects vortex shedding, drag, and lift forces is essential for ensuring subsea pipelines' structural integrity and long-term stability. This paper presents a comprehensive study of the effects of flow velocity on the hydrodynamic behavior of subsea pipelines to improve the design practices and operational guidelines for subsea pipeline systems. This study contributes to optimising subsea pipeline design under varying flow conditions by utilising advanced computational models and experimental data.

II. Method

This study investigates the influence of velocity on the hydrodynamic flow characteristics around subsea pipelines through numerical simulations. The primary objective is understanding how varying flow velocities affect key hydrodynamic parameters, such as pressure distribution, lift and drag coefficients, and vortex shedding around free-span subsea pipelines. To achieve this, a systematic approach is employed, utilizing computational fluid dynamics (CFD) simulations, which are well-established for solving complex fluid flow problems in marine engineering [23].

A. Geometry and Pipeline Setup

The geometry of the subsea pipeline is modelled as a cylindrical structure with a free span above the seabed. The pipeline's diameter and length are selected to represent typical subsea installations, such as oil and gas pipelines. The pipeline is positioned in the simulation domain with an angle relative to the incoming flow of 90°, to capture the most significant flow direction to vortex evolution. The surrounding fluid domain is extended sufficiently to minimize boundary effects, and periodic boundary conditions are applied to simulate continuous flow.

Free span modelling is essential for analysing flow behaviour around unsupported pipeline segments and requires the inclusion of parameters such as pipe diameter, span length, and surrounding flow characteristics. This study uses ANSYS CFD software to model the free-spanning pipe. The model is developed in two dimensions (2D) to provide an initial understanding of flow patterns and vortex formation zones. The pipe geometry is constructed using ANSYS DesignModeler, with boundary conditions and material properties applied according to DNV-RP-F105 [10].

Boundary conditions are applied to simulate physical constraints and flow interactions. The pipe ends are assumed to be fixed to model vibration under flow loading realistically [17]. A refined mesh is applied around the pipe, especially near the span region, to ensure numerical stability and capture detailed vortex structures without excessive computational cost.

To understand the flow field in bedform dynamics interaction with the pipeline, numerical simulations have been undertaken using FLUENT. FLUENT software is an advanced commercial CFD code. It can simulate the flow field of any case and shows good reliability. The flow past an artificial berm and a smooth circular cylinder has been simulated by solving numerically the 2D Navier-Stokes equations for unsteady, incompressible and turbulent flow. The governing equations for the flow around an underwater pipeline are the continuity equation and the momentum equation [24].

$$\frac{\partial u_i}{\partial x_i} = 0 \quad (1)$$

$$\frac{\partial u_i}{\partial t} + u_j\frac{\partial u_i}{\partial x_j} = -\frac{1}{\rho}\frac{\partial p}{\partial x_i} + \frac{\partial(2vS_{ij} - \overline{u_i'u_j'})}{\partial x_j} \quad (2)$$

$$S_{ij} = \frac{1}{2}\left(\frac{\partial u_i}{\partial x_j} + \frac{\partial u_j}{\partial x_i}\right) \quad (3)$$

$$\overline{u_i'u_j'} = v_T\left(\frac{\partial u_i}{\partial x_j} + \frac{\partial u_j}{\partial x_i}\right) + \frac{2}{3}k\delta_{ij} \quad (4)$$

where u_i is the fluid velocity component in the i direction, p is the pressure, ρ is the fluid density, v is the fluid kinetic viscosity, S_{ij} is the mean strain rate tensor, u_i' is the fluctuation of fluid velocity in the i direction, $u_i'u_j'$ is the Reynolds stress tensor, v_T is the turbulence viscosity, and δ_{ij} is the Kronecker delta. Turbulence model $k-\omega$ is one of the most common models used to predict the effects of turbulence [25, 26].

The properties of the pipeline used API 5L – 65 PSL 2 QO/MO grade steel. It has an outer diameter of 16 inches (0.406 m), a wall thickness of 0.56 inches

(0.01422 m), a steel density of 7850 kg/m³ and a Young's modulus of 207,000 MPa. Other parameters include a Poisson's ratio 0.3, with marine growth thickness at 50 mm.

The design current velocities for 1-year, 10-year, and 100-year return periods are 1.01 m/s, 1.43 m/s, and 1.82 m/s, respectively. For the CFD modelling, three different ranges of current velocity of 1.1, 2.5 and 3 m/s, respectively, were selected.

The maximum allowable free span length depends on specific loading conditions experienced during installation, hydrotest, and operational phases. These limits were calculated based on dominant in-line vibration criteria for both single and multiple spans, as shown in Table 1.

TABLE 1.
FREE SPAN SCREENING SUMMARY

Pipeline load condition	Max.Allowable span length (m)	Governing criteria
Installation	17, 36	In-line (single span)
Hydrotest	17,98	In-line (multi span)
Operation uncorroded	11,67	In-line (single span)
Operation corroded	9,62	In-line (single span)

To capture a representative range of seabed topography, a maximum gap of 0.0676 m is selected for the CFD simulation. These values are tested under flow

B. Flow Velocity Variation

To explore the influence of velocity on the hydrodynamic flow, simulations are performed at different inlet velocities, ranging from low to high flow rates. The velocity variation allows the examination of subcritical and supercritical flow regimes, critical in understanding the flow's behavior around the pipeline. The inlet velocity varies in increments from 1 to 3 m/s to accurately represent the velocity's impact on flow structures, with particular attention paid to turbulent flows.

C. Turbulence Modelling

Since the flow around subsea pipelines is highly turbulent, appropriate turbulence models are crucial for accurately simulating the fluid dynamics. The Reynolds-averaged Navier-Stokes (RANS) equations are used in this study, employing the k-ε turbulence model to capture the turbulent effects on the flow [27]. This model is selected due to its computational efficiency and reliability in modelling turbulent flow around cylindrical objects, especially at high Reynolds numbers.

D. Meshing and Grid Independence

A structured computational grid is created for the flow domain to ensure accurate flow simulations around the pipeline. Grid independence studies are performed to ensure the results are not sensitive to the mesh size. The computational grid is refined in the regions near the pipeline surface and the wake, where the flow gradients are expected to be high. The grid resolution is carefully

heading angles of 90° to simulate extreme operational conditions. This approach provides a comprehensive understanding of the VIV risk of the subsea pipeline. chosen to balance computational cost with accuracy, with the final grid ensuring the prediction of vortex shedding patterns and force coefficients with minimal numerical errors [28].

E. Boundary Conditions and Simulation Setup

The boundary conditions for the simulations are set to represent realistic offshore conditions. The pipeline surface is smooth, with a no-slip condition applied to the solid boundaries. The inlet boundary condition is specified with a uniform velocity profile to simulate the approach flow, while the outlet is set as a pressure-outlet with zero-gradient conditions. The sidewalls are treated as symmetry boundaries, allowing the flow to be modelled as two-dimensional. These boundary conditions ensure the flow behaves as it would in a natural subsea environment.

F. Data Collection and Post-Processing

The simulation results are analyzed by extracting key hydrodynamic parameters, including pressure distribution, lift and drag coefficients, and vortex shedding frequency. The lift and drag coefficients are calculated from the forces acting on the pipeline surface using standard aerodynamic formulas [29]. Vortex shedding is analyzed by examining the fluctuating pressures and velocities in the wake region, using vortex identification techniques such as the vorticity magnitude. Post-processing tools, including ParaView, are employed to visualize the flow patterns and vortex structures around the pipeline.

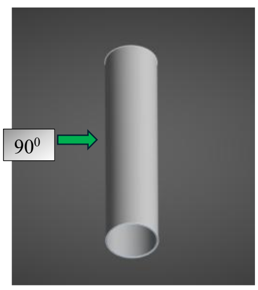

Figure 1. Heading 90°

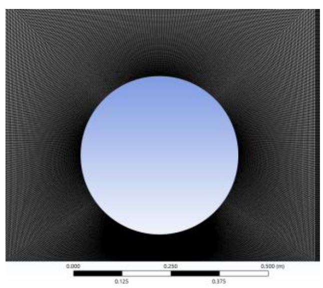

Figure 2. Meshing

III. RESULTS AND DISCUSSION

A. Effect of flow velocity variation on mean flow field

Figure 3 displays the mean flow field at a relatively low incoming flow velocity of 1.1 m/s, where the flow separation occurs symmetrically at the rear of the cylinder. The flow remains relatively stable with minimal vortex formation, and the wake region is narrow and elongated. The recirculation zone is confined near the cylinder, indicating weak boundary layer separation. The contour lines representing velocity gradients show a laminar behavior in the downstream region. This suggests that the inertial forces are not dominant at lower velocities to induce significant flow disturbances or instabilities.

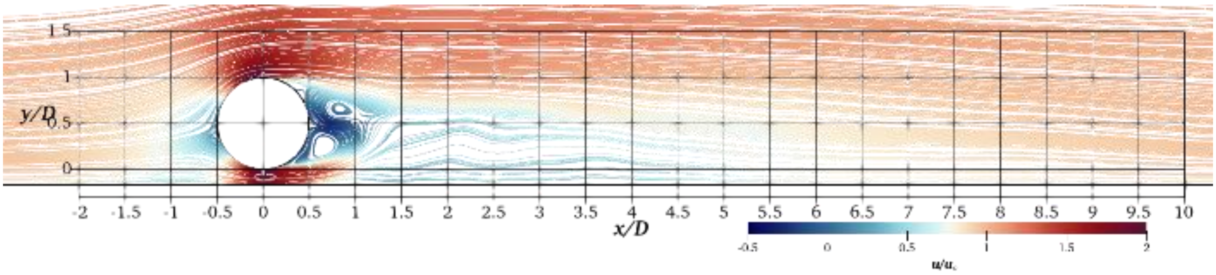

Figure. 3. Mean flow field under flow velocity 1.1 m/s

As the flow velocity increases to 2.5 m/s, as seen in Figure 4, the flow field becomes more unstable. The wake region expands laterally, and vortex shedding becomes apparent. The contours indicate stronger flow separation and a wider zone of recirculation. The increased inertial forces due to higher velocity result in enhanced shear layers on both cylinder sides, leading to periodic vortex formation. This transitional regime marks a shift from steady laminar flow to unsteady flow with the onset of turbulence in the near-wake region.

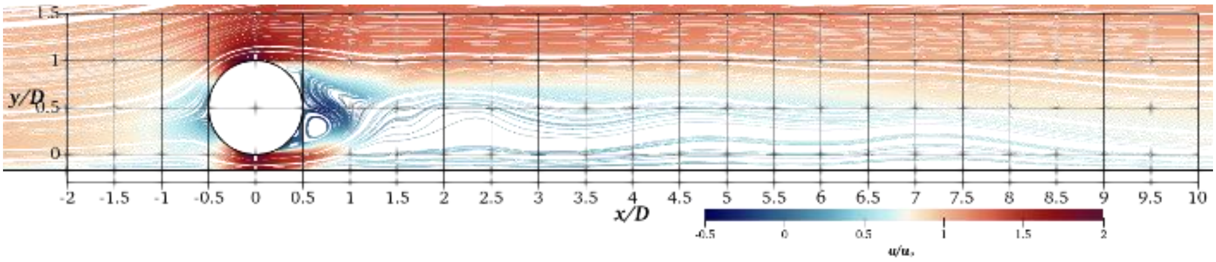

Figure. 4. Mean flow field under flow velocity 2.5 m/s

The flow exhibits more complex and asymmetric behaviour at the highest investigated velocity of 3.0 m/s (Figure 5). The vortex street behind the cylinder fully develops, and the wake widens further than in the previous cases. The shear layers roll up into coherent vortical structures that are convected downstream, forming a distinct Von Kármán vortex street. The increased velocity results in higher Reynolds numbers, promoting turbulent mixing and reducing the length of the steady wake zone. Vortex-induced oscillations that dominate the wake dynamics strongly affect the mean flow.

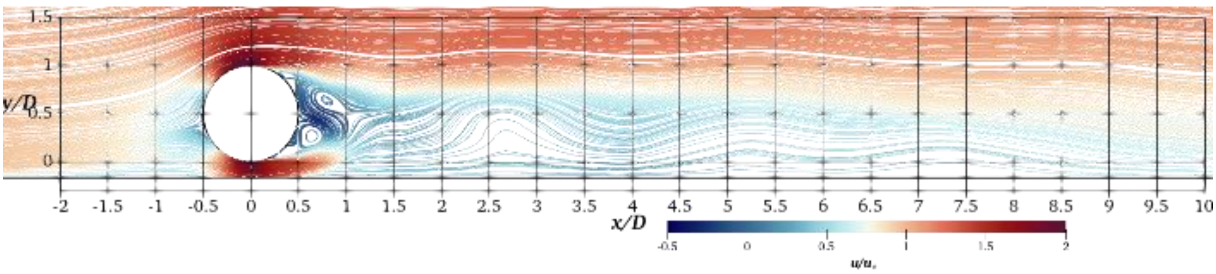

Figure. 5. Mean flow field under flow velocity 3 m/s

The comparison between Figures 3, 4, and 5 clearly illustrates that increasing flow velocity significantly influences the characteristics of the mean flow field around the cylinder. As velocity rises, the transition from laminar to turbulent wake becomes more pronounced, accompanied by increased size and intensity of the separated flow regions. These changes impact drag force and unsteady pressure distributions, critical for engineering applications involving submerged cylindrical structures, such as pipelines or risers.

In summary, the observed flow behavior across the three flow velocities highlights the sensitivity of the wake structure to velocity variation. Lower velocities produce stable and narrow wakes, while higher velocities lead to intense vortex shedding and turbulent wake development. Understanding this transition is crucial in designing and analysing hydrodynamic systems, where flow-induced vibrations and drag forces must be carefully considered for structural integrity and performance optimization.

B. Effect of flow velocity variation on bed shear stress

Figure 6 presents the distribution of bed shear stress (τ) along the normalized streamwise axis (x/D) under three different flow velocities: 1.1 m/s, 2.5 m/s, and 3.0 m/s. Across all velocities, a sharp spike in shear stress is observed at the location corresponding to the front stagnation point of the cylinder (x/D ≈ 0). This peak is attributed to the abrupt flow deceleration upon impact with the cylinder surface, causing elevated wall shear in the immediate vicinity. Among the three conditions, the highest peak is recorded for the 3.0 m/s case, followed by 2.5 m/s and 1.1 m/s, indicating a direct correlation between incoming velocity and peak shear stress.

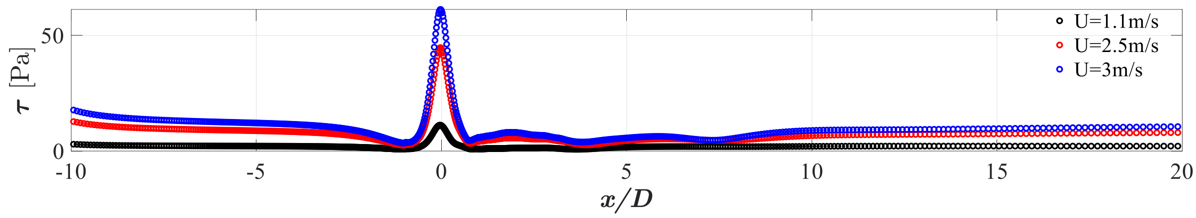

Figure. 6. Bed shear stress in a varying flow velocity

Downstream of the cylinder (x/D > 0), the bed shear stress exhibits oscillatory patterns due to flow separation and vortex shedding. These oscillations are more pronounced at higher velocities, particularly in the 3.0 m/s case, where the turbulence and strength of vortical structures enhance the fluctuation in bed stress. Conversely, the 1.1 m/s condition shows a relatively smoother distribution with lower magnitudes, reflecting a more laminar and stable wake. This pattern highlights the influence of inertial forces and flow unsteadiness in governing bed interaction.

Overall, the data suggest that increased flow velocity significantly elevates bed shear stress's peak and spatial variability. This has important implications for sediment transport and scour potential in practical engineering applications involving submerged pipelines or seabed structures. Understanding the relationship between flow velocity and bed shear behavior is essential for assessing the structural stability and erosion risk in the design of subsea systems.

C. Effect of flow velocity variation on wall pressure

Similar to bed shear stress, Figure 7 depicts the distribution of pressure coefficient (Cp) along the surface of a cylinder subjected to three different flow velocities. The pressure coefficient is defined as $Cp = \frac{(p-p_r)}{0.5\rho U^2}$, where p_r is the pressure at the reference point [26]. The pressure coefficient shows a distinct minimum near the point of flow separation, typically located slightly downstream of the front stagnation point. At x/D = 0, all velocity profiles exhibit a Cp peak, representing the high-pressure region at the frontal impact zone. As flow velocity increases, this frontal Cp peak becomes more compressed and steep, reflecting more substantial inertial effects and more pronounced flow deceleration.

A notable drop in Cp is observed in the post-stagnation region (x/D > 0), indicating flow separation and the formation of a low-pressure wake. The depth and width of this pressure drop are more prominent at higher velocities, especially at 3.0 m/s, where the Cp minimum reaches its lowest value. This is consistent with developing a stronger, more unsteady wake at higher Reynolds numbers. The recovery of pressure downstream is also slower in high-velocity conditions, indicating prolonged vortex activity and delayed pressure reattachment along the wall.

The overall trend highlights a strong dependence of pressure distribution on the incoming flow velocity. Higher velocities amplify the adverse pressure gradient around the cylinder, intensifying separation and contributing to larger unsteady forces on the structure. These variations in Cp are critical for evaluating flow-induced pressure loading, potential fatigue, and hydrodynamic performance in offshore engineering systems, especially those involving submerged cylindrical elements like risers and pipelines.

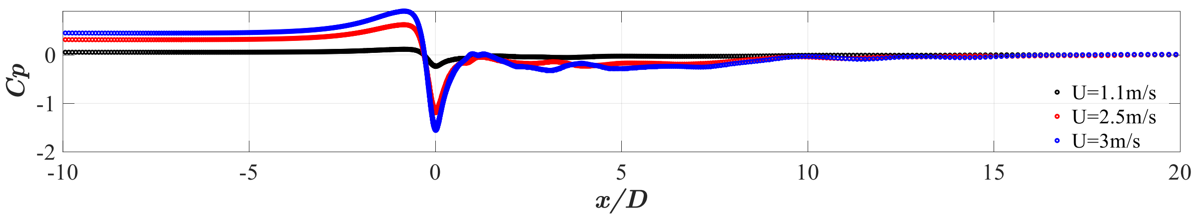

Figure. 7. Pressure coefficient along the wall in a varying flow velocity

D. Effect of flow velocity variation on pipe pressure

Figure 8 illustrates the distribution of pressure coefficient (Cp) along the circumference of a pipe surface under varying flow velocities. The horizontal axis represents the angular position (α/π) around the pipe, ranging from the front stagnation point (α/π = 0) to the rear side (α/π = 2). At the front (α/π ≈ 0), all three flow conditions show a Cp maximum, corresponding to the stagnation point where fluid decelerates and pressure peaks. A steep drop follows this peak as the fluid accelerates around the curved surface of the pipe.

As the flow progresses along the surface, the Cp decreases due to boundary layer acceleration and adverse pressure gradient effects. The lowest Cp values occur near α/π ≈ 1.3, where flow separation typically begins. The negative Cp values are more pronounced at higher flow velocities, especially at 3.0 m/s, indicating a more substantial suction effect caused by increased inertial forces and earlier separation. Furthermore, the flow at higher velocities exhibits more irregularities and fluctuations in the Cp profile, suggesting greater unsteadiness and dynamic pressure variation around the pipe.

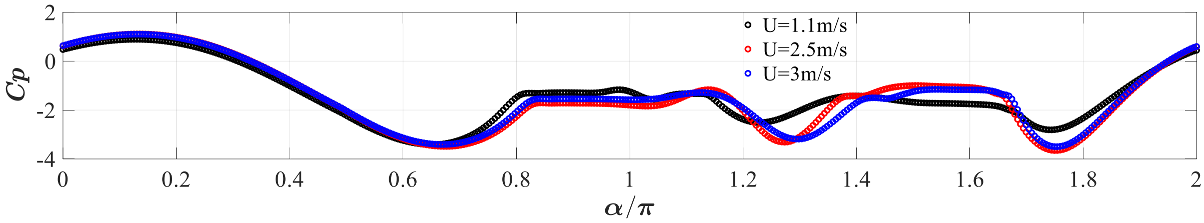

Figure 8. Pressure coefficient along the pipe in a varying flow velocity

The pattern confirms that increasing flow velocity significantly amplifies the pressure differences across the pipe surface. These variations in Cp influence the net drag and lift forces acting on the pipe, which are crucial factors in submerged pipelines' hydrodynamic performance and structural design. In particular, stronger pressure gradients and earlier flow separation at higher velocities may lead to intensified vortex shedding and fluctuating pressure loads, which must be accounted for in offshore and subsea pipeline stability assessments.

E. Effect of flow velocity variation on velocity profile

Figure 9 illustrates the evolution of streamwise velocity profiles (u) at multiple downstream sections behind a cylindrical pipe subjected to three distinct flow velocities. The vertical axis represents the normalized vertical position (y/D), while the horizontal axis shows the streamwise velocity (u) in m/s. Across all profiles, flow velocity is significantly reduced in the near-wake region, forming a clear velocity deficit directly behind the cylinder. The extent of this deficit is largest for the highest incoming velocity (3.0 m/s), indicating a more pronounced disturbance and wider wake zone due to increased inertial effects and turbulent vortex shedding.

As the distance from the cylinder increases, the velocity profiles gradually recover towards the freestream condition, although the recovery is notably slower for higher flow velocities. At 1.1 m/s, the profiles demonstrate a relatively narrow wake and quicker velocity restoration, reflecting a more laminar flow with weaker vortex formation. In contrast, the profiles for 2.5 m/s and especially 3.0 m/s show delayed recovery and stronger asymmetry in the velocity field, consistent with enhanced turbulent mixing and energy dissipation in the far wake. This observation confirms that the Reynolds number strongly influences wake persistence.

The variation in velocity profiles concerning downstream location and flow velocity provides critical insight into flow reattachment and turbulence development. In practical applications such as subsea pipeline analysis or marine structure design, understanding the velocity field is essential for predicting vortex-induced vibrations, local scour, and hydrodynamic loading. The results suggest that higher flow velocities intensify wake turbulence and extend its spatial influence, necessitating careful consideration in engineering analysis and mitigation strategies.

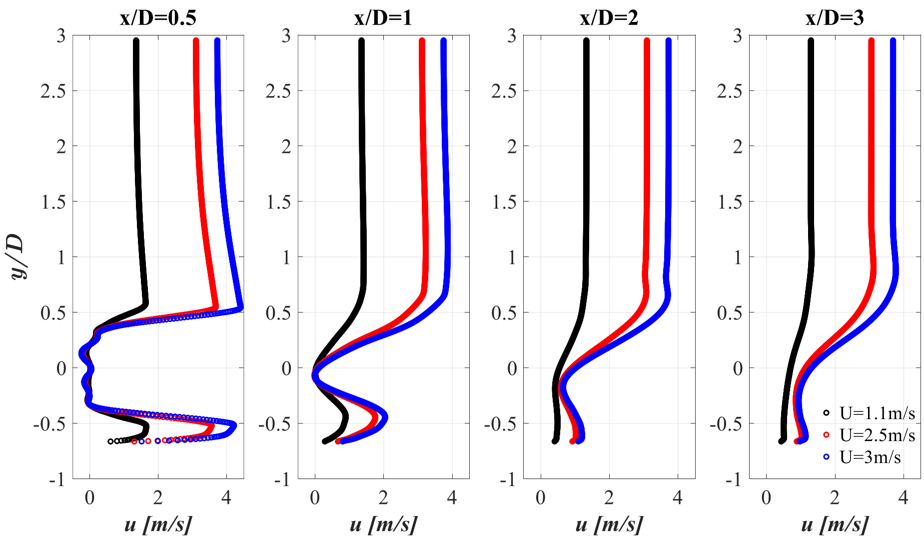

Figure. 9. Velocity profile in different locations at the downstream side of the pipe under variation of velocity

Figure 10 presents the streamwise velocity profiles normalized by the freestream velocity (u_0) at different downstream positions behind a cylindrical pipe for three flow velocities (1.1 m/s, 2.5 m/s, and 3.0 m/s). The normalization provides a clearer comparative insight into the relative wake behavior, independent of absolute velocity magnitudes. All profiles demonstrate a pronounced velocity deficit in the wake center, especially in the regions closest to the pipe. As the flow develops downstream, the deficit diminishes gradually, and the velocity recovers toward the normalized freestream value ($u/u_0 \approx 1$). The wake width and depth remain more substantial in higher velocity cases, highlighting the stronger wake influence at increased Reynolds numbers.

Compared to Figure 9, where absolute velocities vary significantly among the flow cases, the normalized profiles in Figure 10 reveal a more unified representation of wake structure. At normalized scale, it becomes evident that the general shape and asymmetry of the velocity profiles are preserved across different flow velocities. However, subtle differences can still be observed in the wake recovery rate—slower for 3.0 m/s and faster for 1.1 m/s. This suggests that despite velocity normalization, higher velocity flows retain their turbulent character and require longer distances to fully stabilize, as indicated by persistent deficits near the centerline ($y/D \approx 0$).

The comparison between Figures 9 and 10 emphasizes the importance of using absolute and normalized velocity profiles to analyse wake behavior. While absolute profiles inform about the scale of velocity changes and drag-related impacts, normalized profiles better reveal the structural evolution and shape of the wake. From an engineering standpoint, normalized data is particularly useful in developing dimensionless correlations and predicting wake effects for different flow conditions without repeating full-scale simulations. The results reinforce the role of flow velocity in governing the turbulence intensity and wake persistence downstream of bluff bodies such as submerged pipelines.

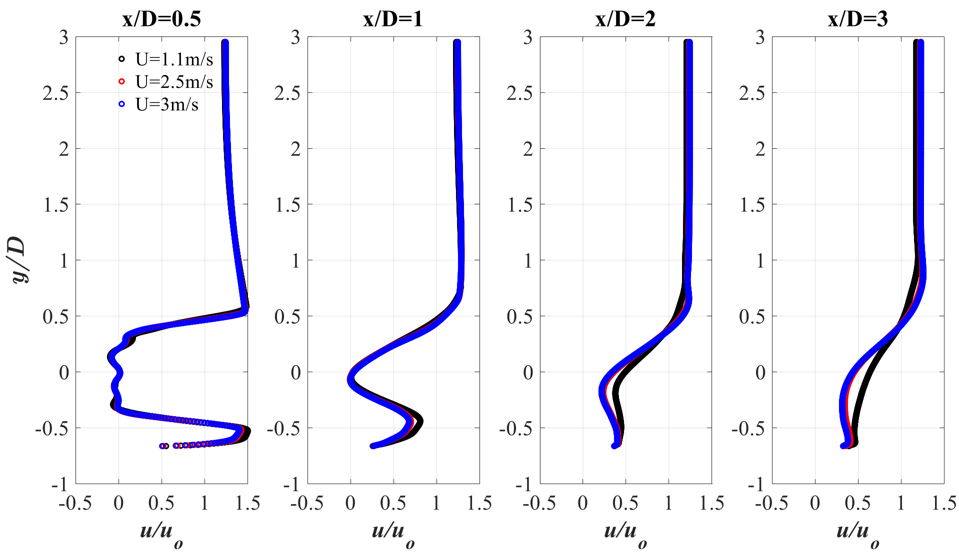

Figure. 10. Velocity profile normalized by the mean flow in different locations at the downstream side of the pipe under variation of velocity

IV. Conclusion

This study comprehensively examined the influence of flow velocity on hydrodynamic behavior around subsea pipelines using computational fluid dynamics (CFD). The simulation results show that increasing flow velocity significantly alters the flow field structure, transitioning from a stable laminar wake at low velocity to an unsteady, turbulent vortex street at higher velocities. The mean flow field becomes increasingly asymmetric and unstable as velocity rises, with enhanced vortex shedding and broader wake regions, particularly at 3.0 m/s.

Increased flow velocity amplifies bed shear stress and wall pressure gradients around the pipe. The peak bed shear stress was found at the stagnation point, with higher velocities producing larger oscillations downstream due to intensified vortex dynamics. Pressure coefficient profiles showed more negative values and delayed recovery at higher velocities, indicating stronger adverse pressure gradients and more pronounced flow separation. These effects contribute to fluctuating hydrodynamic loads critical in fatigue analysis and pipeline integrity.

Furthermore, both absolute and normalized velocity profiles revealed that higher flow velocities deepen the velocity deficit in the wake and slow its recovery. Normalized profiles confirmed the persistence of wake asymmetry at high Reynolds numbers. These findings underscore the critical role of flow velocity in governing vortex-induced vibrations (VIV), hydrodynamic loading, and scour potential. Therefore, careful consideration of velocity effects is essential in designing and analysing subsea pipelines to ensure long-term structural performance under varying marine current conditions.

ACKNOWLEDGEMENT

The authors would like to acknowledge the support fund from the Internal Research Grant, Lembaga

Penelitian dan Pengabdian Masyarakat, Institut Teknologi Kalimantan (No. 13341/IT10.L1/PPM.04/2025) through research funding.

References

[1] M. Randolph and S. Gourvenec, *Offshore Geotechnical Engineering*, 1st ed. ed. CRC Press, 2011.
[2] Q. Bai and Y. Bai, *Subsea pipeline design, analysis, and installation*. gulf professional publishing, 2014.
[3] S. K. Chakrabarti, "Handbook of Offshore Engineering, Elsevier," *The Netherlands,* 2005.
[4] A. C. Palmer and R. A. King, "Subsea pipeline engineering," *(No Title),* 2008.
[5] A. A. Olsen, "Subsea Pipeline Systems."
[6] J. Fredsøe, "Pipeline–Seabed Interaction," (in En), *Journal of Waterway, Port, Coastal, and Ocean Engineering,* vol. 142, no. 6, p. 03116002, 2016/11/01/ 2016, doi: 10.1061/(ASCE)WW.1943-5460.0000352.
[7] M. Mohaddes Pour and S. S. Razavi Taheri, "Free Span Analysis for Submarine Pipelines," *Shock and Vibration,* vol. 2021, no. 1, p. 9305129, 2021.
[8] Y. Bai, *Deepwater flexible risers and pipelines*. John Wiley & Sons, 2020.
[9] A. A. Shittu, F. Kara, A. Aliyu, and O. Unaeze, "Review of pipeline span analysis," *World Journal of Engineering,* vol. 16, no. 1, pp. 166-190, 2019.
[10] DNV, "Free spanning pipelines," *Recommended practice DNV-RPF105,* pp. 1-46, 2006.
[11] S. H. F. Leckie, "Scour and sedimentation around subsea pipelines," Doctor of Philosophy, School of Civil and Resource Engineering, The University of Western Australia, The University of Western Australia, 2016.
[12] B. L. Jensen, B. M. Sumer, H. R. Jensen, and J. Fredsoe, "Flow around and forces on a pipeline near a scoured bed in steady current," 1990.
[13] P. Bearman and M. Zdravkovich, "Flow around a circular cylinder near a plane boundary," *Journal of Fluid Mechanics,* vol. 89, no. 1, pp. 33-47, 1978.
[14] Z. Zhang, Y. Guo, Y. Yang, B. Shi, and X. Wu, "Scale model experiment on local scour around submarine pipelines under bidirectional tidal currents," *Journal of Marine Science and Engineering,* vol. 9, no. 12, p. 1421, 2021.
[15] B. Zhang, H. An, S. Draper, H. Jiang, L. Cheng, and X. Zhao, "Three-Dimensional Flow Around a Span Shoulder of a Pipeline/Cable: Insight From Experiments Combined With Numerical Modelling," in *International Conference on Offshore Mechanics and Arctic Engineering*, 2024, vol. 87844: American Society of Mechanical Engineers, p. V006T08A023.
[16] B. Zhang, H. An, S. Draper, H. Jiang, and L. Cheng, "Numerical Simulations of Three-Dimensional Scour Below Subsea Pipelines/Cables Under Steady Current Conditions," in *International Conference on Offshore Mechanics and Arctic Engineering*, 2023, vol. 86892: American Society of Mechanical Engineers, p. V007T08A030.
[17] S. A. Shittu, *Numerical Simulation of Vortex-induced Vibration of Free Spanning Underwater Pipeline Close to the Seabed*. The University of Manchester (United Kingdom), 2022.
[18] F. Xiao and H.-C. Chen, "CFD simulation of vortex–induced vibrations of free span pipelines including pipe-soil interactions," in *ISOPE International Ocean and Polar Engineering Conference*, 2015: ISOPE, pp. ISOPE-I-15-267.
[19] B. M. Bossio V, A. J. Blanco A, and E. L. Casanova M, "Numerical modeling of the dynamical interaction between slug flow and vortex induced vibration in horizontal submarine pipelines," *Journal of Offshore Mechanics and Arctic Engineering,* vol. 136, no. 4, p. 041803, 2014.
[20] A. Ragab, W. Brandstaetter, and S. Shalaby, "CFD-simulation of multiphase flows in horizontal and inclined pipelines," *Oil, Gas (Hamburg),* vol. 34, 2008.
[21] R. H. Willden and J. M. R. Graham, "CFD simulations of the vortex-induced vibrations of model riser pipes," in *International Conference on Offshore Mechanics and Arctic Engineering*, 2005, vol. 41979, pp. 837-846.
[22] D. Liang, L. Cheng, and K. Yeow, "Numerical study of the Reynolds-number dependence of two-dimensional scour beneath offshore pipelines in steady currents," *Ocean Engineering,* vol. 32, no. 13, pp. 1590-1607, 2005.
[23] A. N. Patankar and G. Mandal, "The packing of solid particles: a review," *Transactions of the Indian Ceramic Society,* vol. 39, no. 4, pp. 109-119, 1980.
[24] Z. Zhang, B. Shi, Y. Guo, and L. Yang, "Numerical investigation on critical length of impermeable plate below underwater pipeline under steady current," *Science China Technological Sciences,* vol. 56, pp. 1232-1240, 2013.
[25] L. Dongfang and C. Liang, "Numerical modeling of flow and scour below a pipeline in currents, Part I: Flow simulation," *Coastal Engineering,* vol. 52, pp. 25-42, 2004.
[26] H. An, L. Cheng, and M. Zhao, "Numerical simulation of a partially buried pipeline in a permeable seabed subject to combined oscillatory flow and steady current," *Ocean engineering,* vol. 38, no. 10, pp. 1225-1236, 2011.
[27] B. E. Launder and D. B. Spalding, "The numerical computation of turbulent flows," in *Numerical prediction of flow, heat transfer, turbulence and combustion*: Elsevier, 1983, pp. 96-116.
[28] P. Chakraborty, S. Balachandar, and R. J. Adrian, "Kinematics of local vortex identification criteria," *Journal of visualization,* vol. 10, no. 2, pp. 137-140, 2007.
[29] E. L. Houghton and P. W. Carpenter, *Aerodynamics for engineering students*. Elsevier, 2003.